

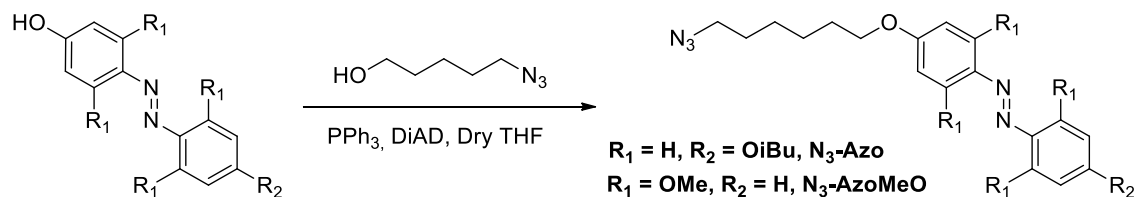
Supplementary Materials

Polymeric Self-Assemblies Based on tetra-*ortho*-Substituted Azobenzene as Visible Light Responsive Nanocarriers

Alejandro Roche ¹, Luis Oriol ¹, Rosa M. Tejedor ^{1,2,*} and Milagros Piñol ^{1,*}

1. Synthesis and characterization of N₃-Azo and N₃-AzoOMe

Azide azobenzenes were synthesized as illustrated in Scheme S1 from the corresponding 4-hydroxyazobencenes *via* Mitsunobu reaction with 6-azidohexan-1-ol. 4-Isobutoxy-4'-hydroxyazobenzene [1], 2,2',5,5'-tetramethoxy-4-hydroxy-azobenzene [2] and 6-azidohexan-1-ol [3] were synthesized according to previously reported procedures.



Scheme S1. General Synthesis of Azides N₃-Azo y N₃-AzoOMe

1.1. Synthesis and characterization of 4-isobutoxy-4'-(6-azidohexyl-1-oxy)azobenzene (N₃-Azo)

4-Isobutoxy-4'-hydroxyazobenzene (1.50 g, 5.54 mmol), 6-azidohexanol (786 mg, 5.54 mmol) and diisopropyl azodicarboxylate (DIAD) (1.12 g, 5.54 mmol) were dissolved in dry THF (50 mL) under Ar atmosphere and cooled down in an acetone-ice bath. Then, a triphenylphosphine (PPh₃) (1.45 g, 5.54 mmol) solution in anhydrous THF (10 mL) was added dropwise. The reaction mixture was stirred for 24 h. Solvent was evaporated to dryness and the product purified by recrystallization in ethanol. Product was isolated by filtration as a pale orange solid. Yield 80%. FTIR (KBr disk, cm⁻¹): 3050 (Csp²-H), 2938 (Csp³-H), 2102 (N₃), 1560 (CAr-CAr), 1471 (N=N), 1239 (C-O). ¹H NMR [400 MHz, CDCl₃, δ, ppm]: 7.94 - 7.79 (m, 4H), 7.07 - 6.91 (m, 4H), 4.03 (t, J = 6.4 Hz, 2H), 3.80 (d, J = 6.6 Hz, 2H), 3.29 (t, J = 6.8 Hz, 2H), 2.17 - 2.06 (m, 1H), 1.90 - 1.78 (m, 2H), 1.72 - 1.58 (m, 2H), 1.57 - 1.38 (m, 4H), 1.05 (d, J = 6.8 Hz, 6H). ¹³C NMR [100 MHz, CDCl₃, ppm]: 161.45, 161.15, 147.15, 147.05, 124.32, 114.82, 114.18, 74.81, 68.16, 51.51, 29.22, 28.93, 28.42, 26.65, 25.80, 19.37.

1.2. Synthesis and characterization of 2,2',5,5'-tetramethoxy-4-oxo-(6''-azidohexyl-1-oxy) azobenzene (N₃-AzoOMe)

2,2',5,5'-Tetramethoxy-4-hydroxyazobenzene, (400 mg, 1.26 mmol), DPTS (146 mg, 0.51 mmol) and 6-azidohexanoic acid (239 mg, 1.52 mmol) were dissolved in dry dichloromethane (10

mL) under Ar atmosphere. The flask was cooled in an acetone-ice bath. Then, EDC (290 mg, 1.52 mmol) was added under Ar atmosphere. After half an hour, the ice bath was removed and the reaction was stirred for 72 h. Crude reaction was diluted with dichloromethane (100 mL) and washed with water ($2 \times$ 100 mL) and brine (100 mL). The organic phase was dried over anhydrous MgSO₄, filtered off and evaporated. The residue was purified by silica column chromatography, using dichloromethane/ethyl acetate (8/2) as eluent. Yield 45%. FTIR (KBr, ν_{max} /cm⁻¹): 3009 (Csp²-H), 2942 (Csp³-H), 2092 (N₃), 1581 (CAr-CAr), 1472 (N=N), 1255 (C-O). NMR ¹H [400 MHz, CDCl₃, δ (ppm)]: 7.18 (t, J = Hz, 1H), 6.65 (d, J = Hz, 2H), 6.21 (s, 2H), 4.01 (t, J = Hz, 2H), 3.87 (s, 6H), 3.84 (s, 6H), 3.30 (t, J = Hz, 2H), 1.90 - 1.75 (m, 2H), 1.73 - 1.60 (m, 2H), 1.60 - 1.39 (m, 4H). NMR ¹³C [100 MHz, CDCl₃, δ (ppm)]: 161.03, 154.49, 152.28, 134.82, 128.71, 128.52, 105.2, 91.92, 67.75, 56.62, 51.33, 29.06, 28.75, 26.49, 25.64.

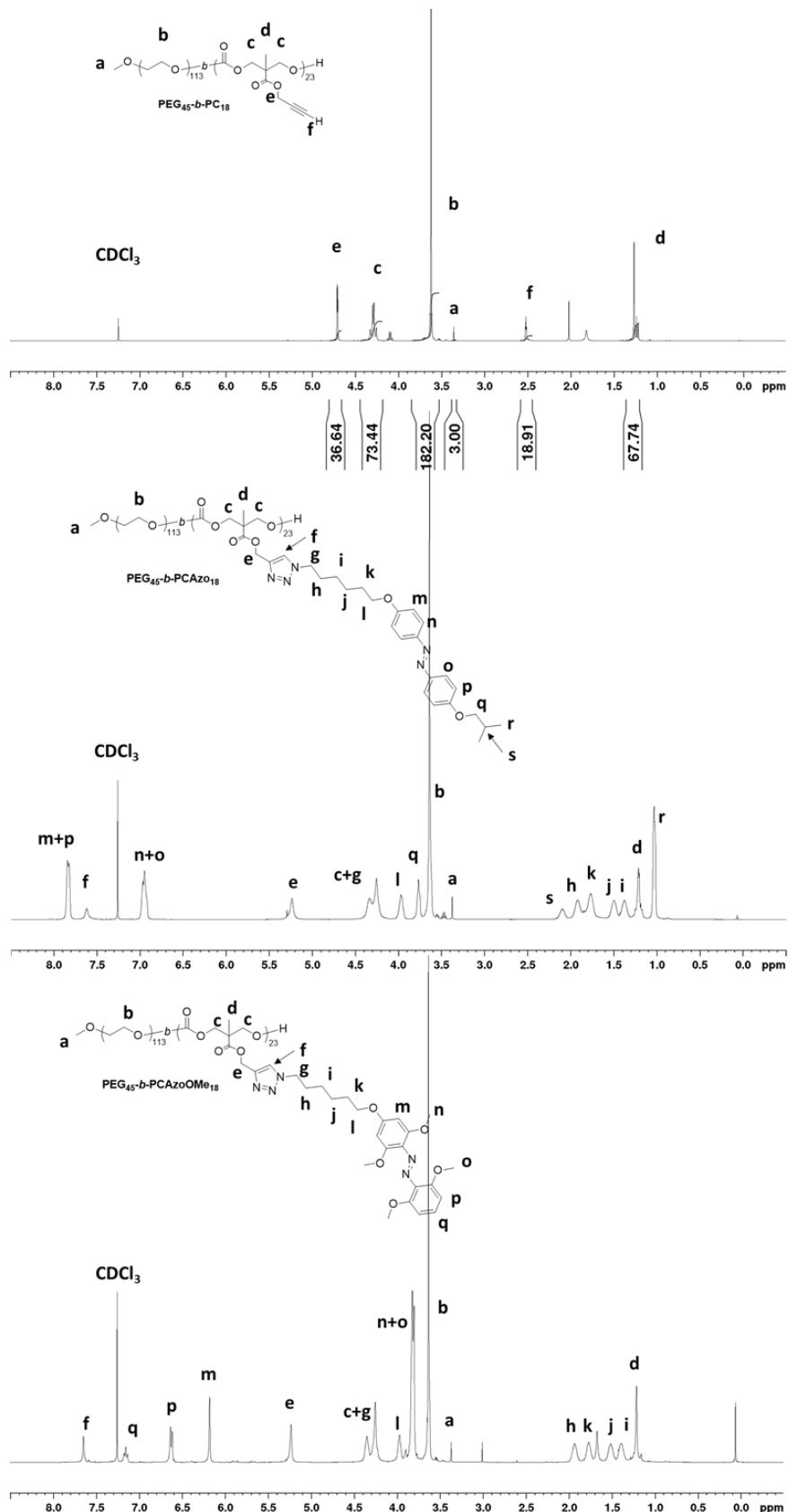


Figure S1. $^1\text{H-NMR}$ (400 MHz, CDCl_3) spectra of (from top to bottom) $\text{PEG}_{45}-b\text{-PC}_{18}$, $\text{PEG}_{45}-b\text{-PCAzo}_{18}$ and $\text{PEG}_{45}-b\text{-PCAzoOMe}_{18}$.

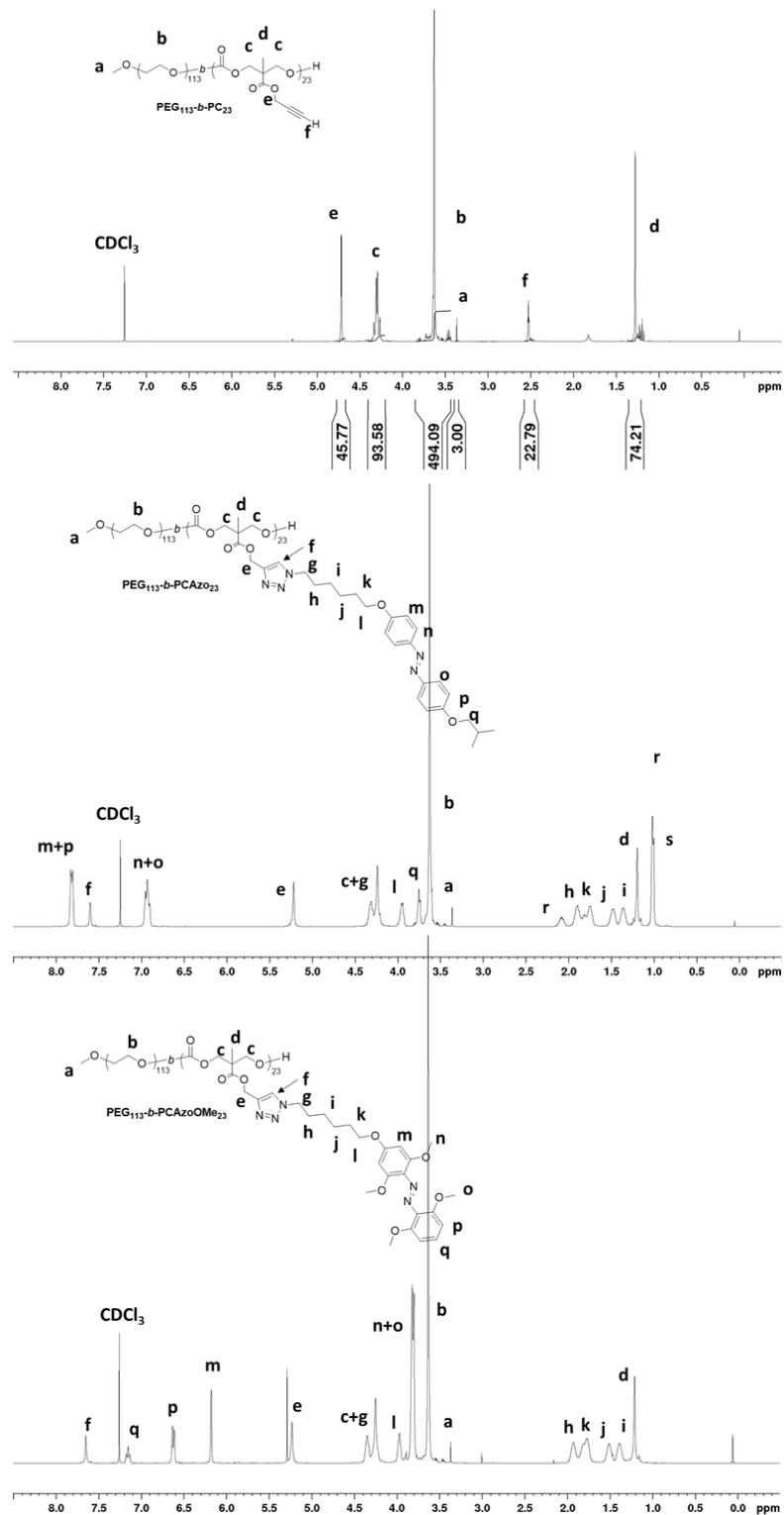


Figure S2. ^1H -NMR (400 MHz, CDCl₃) spectra of (from top to bottom) PEG₁₁₃-*b*-PC₂₃, PEG₁₁₃-*b*-PCAzO₂₃ and PEG₁₁₃-*b*-PCAzOMe₂₃.

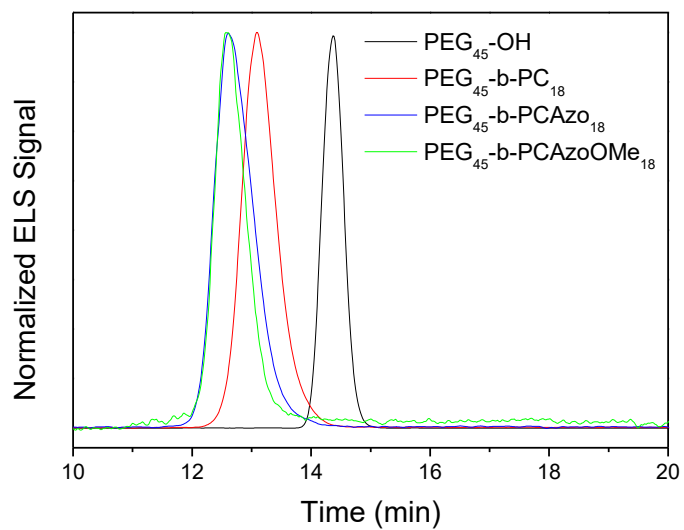


Figure S3. SEC traces for PEG₄₅-OH, PEG₄₅-*b*-PC₁₈, PEG₄₅-*b*-PCAzo₁₈ and PEG₄₅-*b*-PCAzoOMe₁₈.

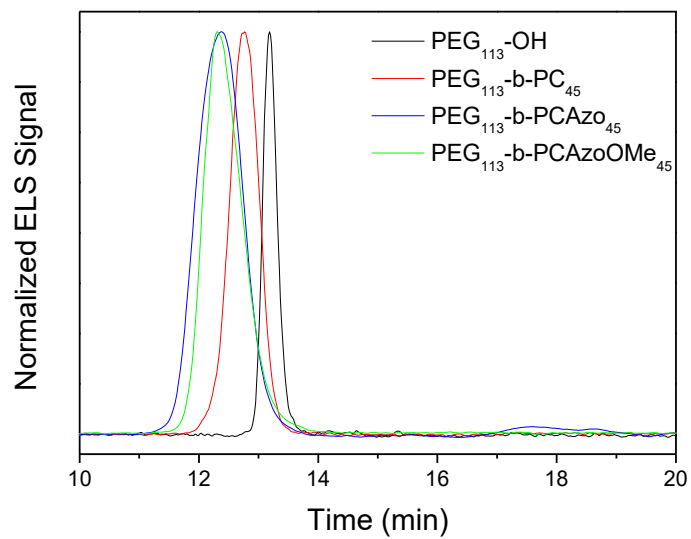


Figure S4. SEC traces for PEG₁₁₃-OH, PEG₁₁₃-*b*-PC₂₃, PEG₁₁₃-*b*-PCAzo₂₃ and PEG₁₁₃-*b*-PCAzoOMe₂₃.

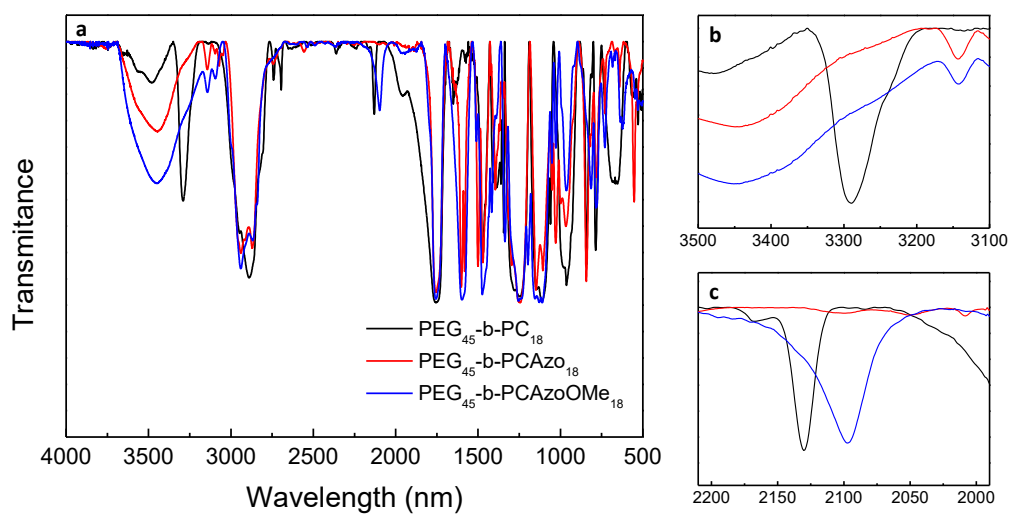


Figure S5. PEG₄₅-b-PC₁₈, PEG₄₅-b-PCAzo₁₈ and PEG₄₅-b-PCAzoOMe₁₈ FTIR spectrum (KBr disk) (a), and zoom to Csp-H zone (b) and Csp-Csp zone (c).

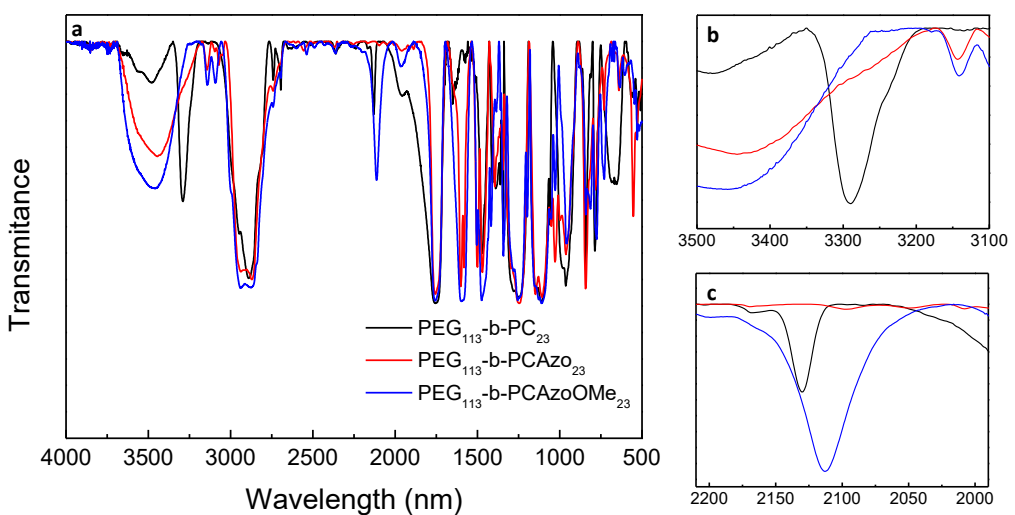


Figure S6: PEG₁₁₃-b-PC₂₃, PEG₁₁₃-b-PCAzo₂₃ and PEG₁₁₃-b-PCAzoOMe₂₃ FTIR spectrum (KBr disk) (a), and zoom to Csp-H zone (b) and Csp-Csp zone (c).

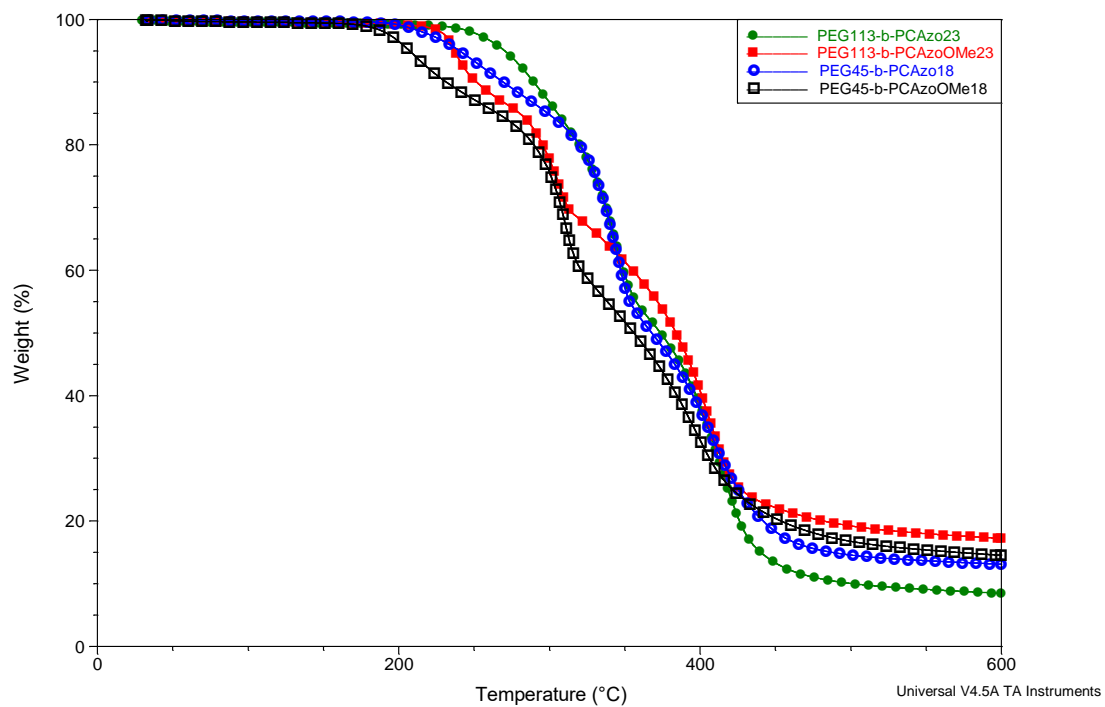


Figure S7. TGA curves registered at $10\text{ }^{\circ}\text{C min}^{-1}$ heating rate under nitrogen atmosphere.

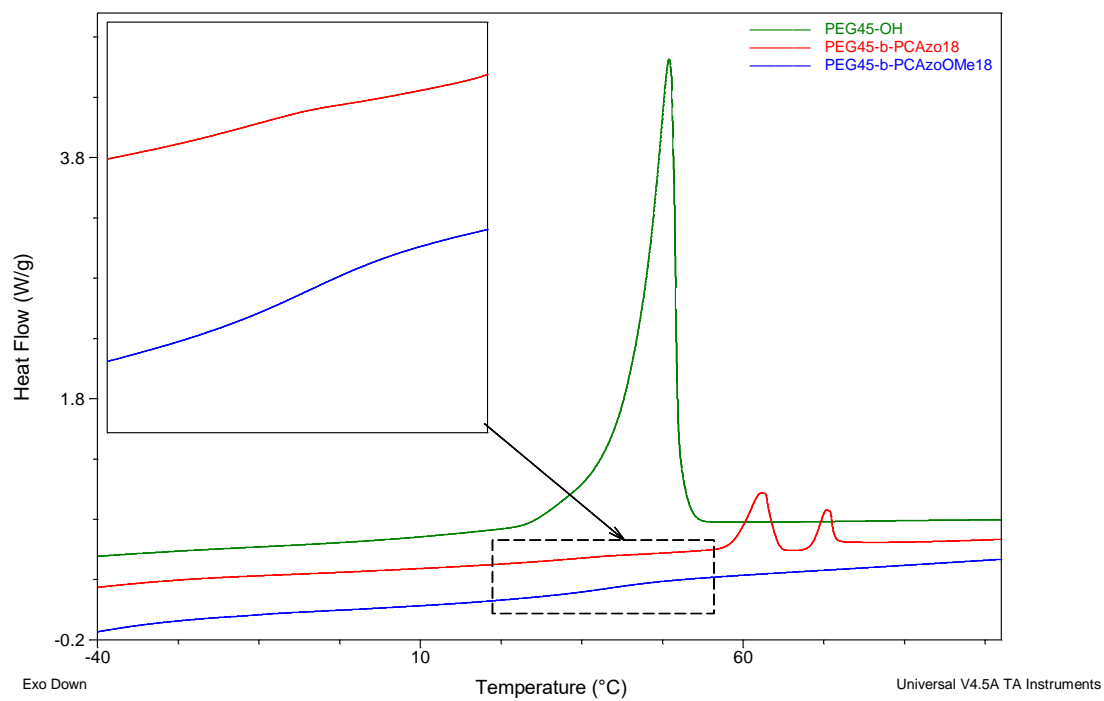
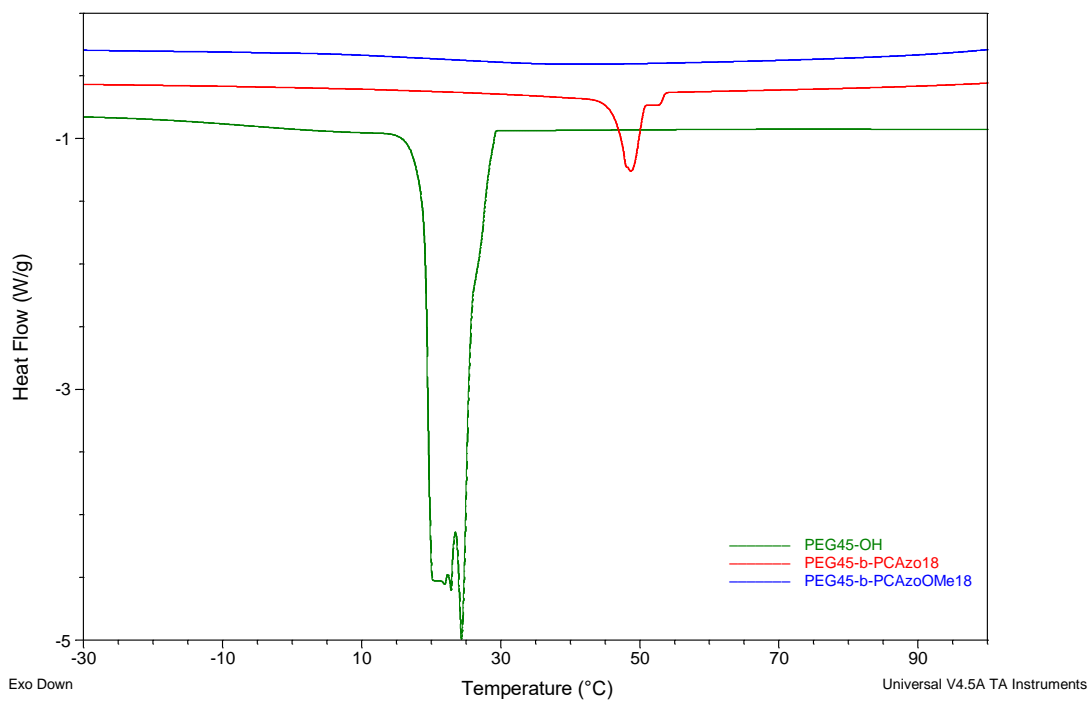


Figure S8. DSC curves registered on cooling (above) and subsequent heating (below) at a 10 °C min⁻¹ scanning rate of PEG₄₅-OH, PEG₄₅-b-PCAzo₁₈ and PEG₄₅-b-PCAzoOMe₁₈.

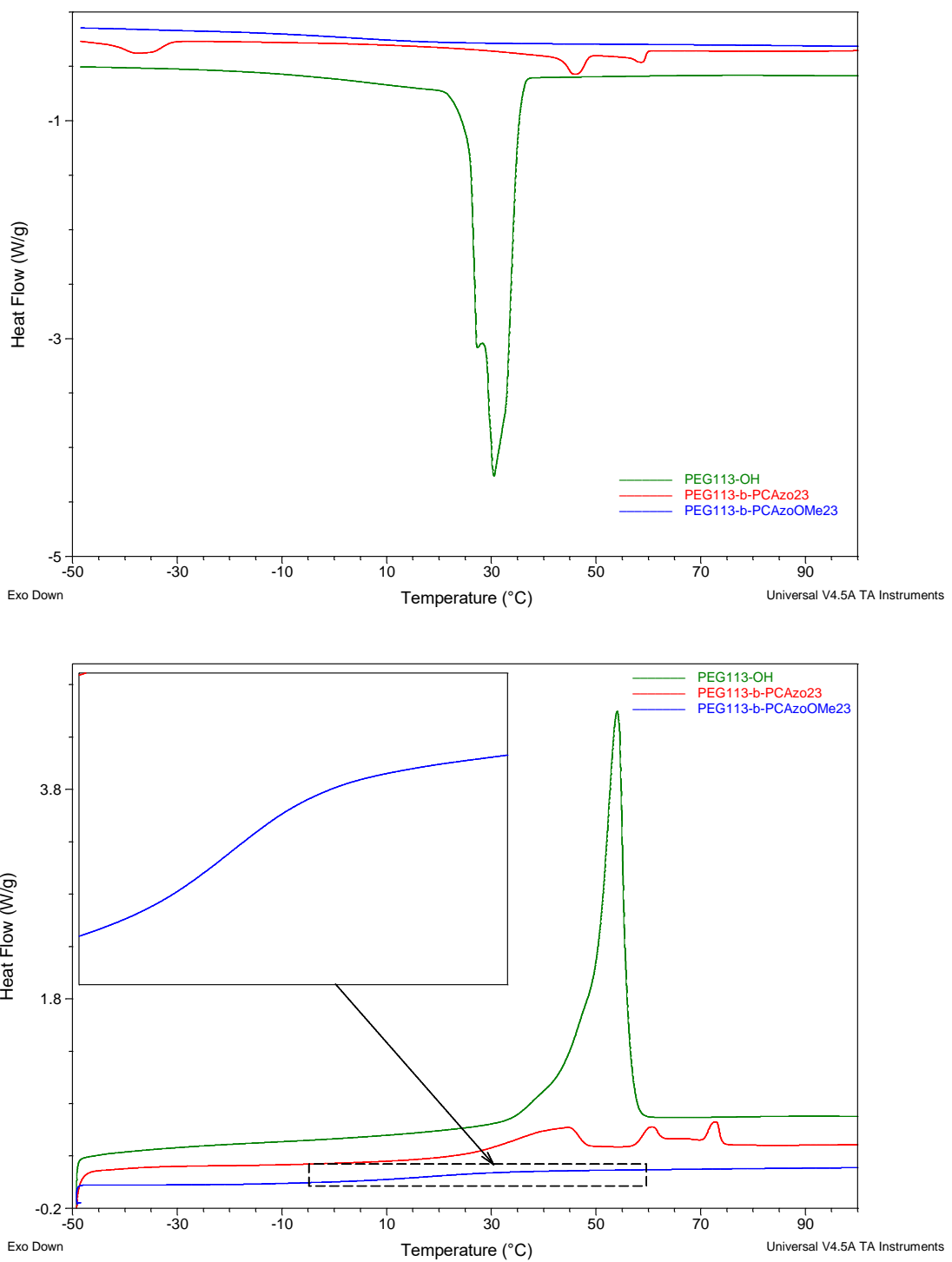


Figure S9. DSC curves registered on cooling (above) and subsequent heating (below) at a 10 °C min⁻¹ scanning rate of PEG₁₁₃-OH, PEG₁₁₃-b-PCAzO₂₃ and PEG₁₁₃-b-PCAzO(Me)₂₃.

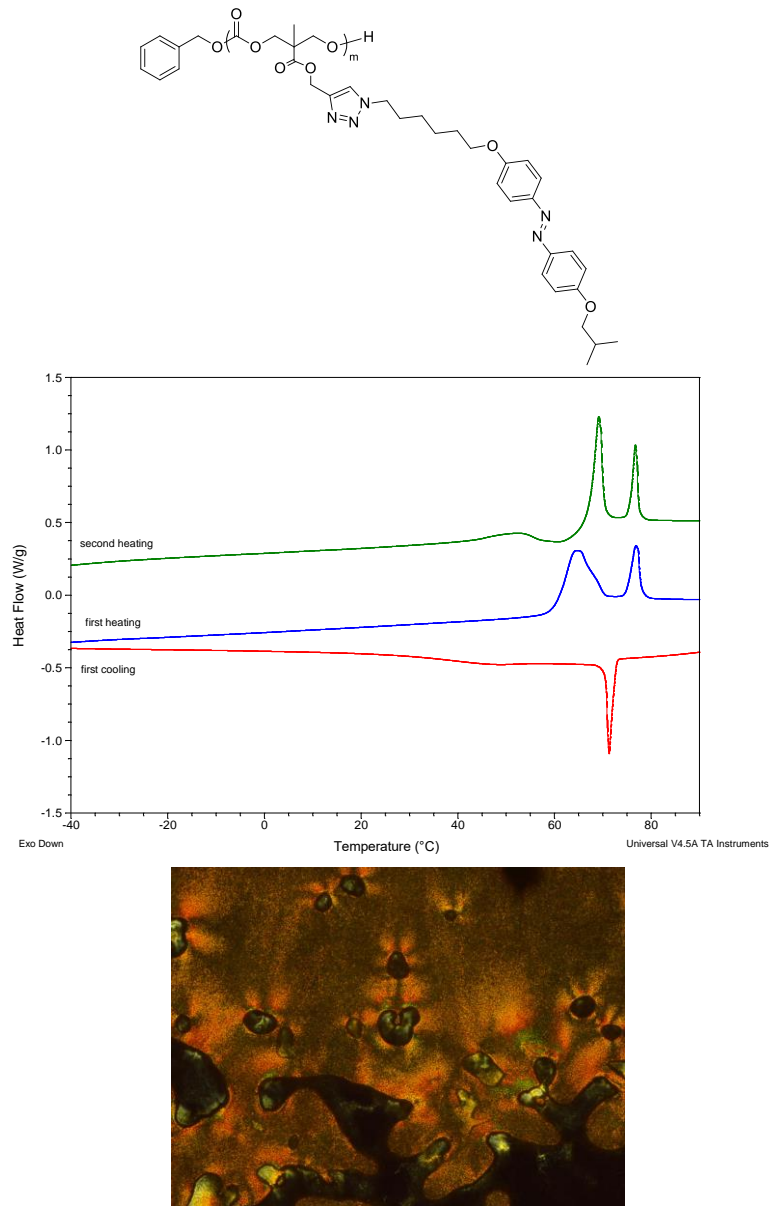


Figure S10. Structure of PCAzo (above), DSC curves registered at a $10\text{ }^{\circ}\text{C min}^{-1}$ scanning rate (middle) and POM image (below) captured at $73\text{ }^{\circ}\text{C}$ for homopolymer PCAzo. From the DSC scans, it was deduced that the isotropic liquid the mesophase vitrifies on cooling. On subsequent heating, the glass transition was measured at $46\text{ }^{\circ}\text{C}$ followed by a cold crystallization process. Two endothermic transitions at $69\text{ }^{\circ}\text{C}$ ($\Delta H = 5.4\text{ kJ}$ per mole of repeating unit) and $77\text{ }^{\circ}\text{C}$ ($\Delta H = 2.5\text{ kJ}$ per mole of repeating unit) were registered corresponding to melting of the crystalline fraction and to the mesophase-to-isotropic liquid transition, respectively. No clearly identifiable textures were observed even after prolonged thermal annealing of the sample.

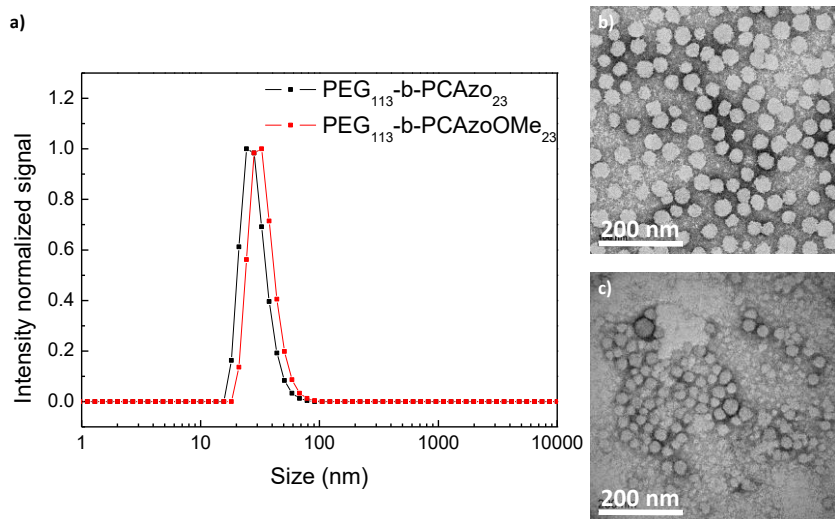


Figure S11. Analysis of the self-assembled structures of PEG_{113} amphiphilic block copolymers series. (a) DLS distribution curves of $\text{PEG}_{113}\text{-}b\text{-PCAzO}_{23}$ and $\text{PEG}_{113}\text{-}b\text{-PCAzOOME}_{23}$. TEM image of (b) $\text{PEG}_{113}\text{-}b\text{-PCAzO}_{23}$ and (c) $\text{PEG}_{113}\text{-}b\text{-PCAzOOME}_{23}$

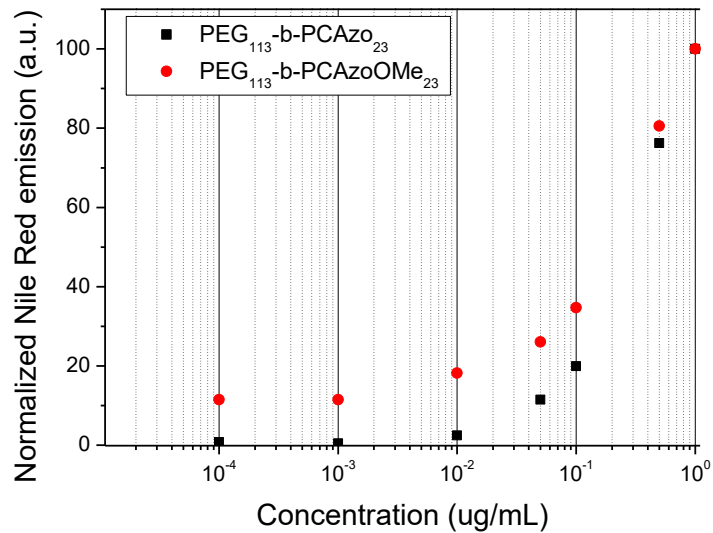


Figure S12. Normalized fluorescence emission of Nile Red at 606 nm ($\lambda_{\text{exc}} = 550$ nm) versus the $\text{PEG}_{113}\text{-}b\text{-PCAzO}_{23}$ and $\text{PEG}_{113}\text{-}b\text{-PCAzOOME}_{23}$ concentration. CAC was determined from the intersection of the two extrapolated lines.

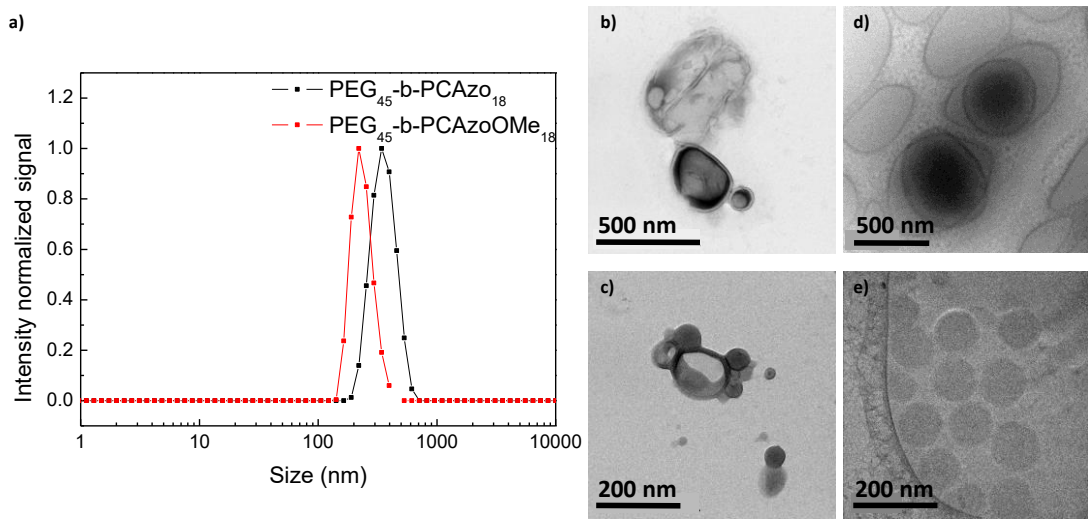


Figure S13. Analysis of the self-assembled structures of PEG₄₅ amphiphilic block copolymers series. (a) DLS distribution curves of PEG₄₅-b-PCAzo₁₈ and PEG₄₅-b-PCAzoOMe₁₈. TEM images of (b) PEG₄₅-b-PCAzo₁₈ and (c) PEG₄₅-b-PCAzoOMe₁₈. Cryo-TEM image of (d) PEG₄₅-b-PCAzo₁₈ and (e) PEG₄₅-b-PCAzoOMe₁₈

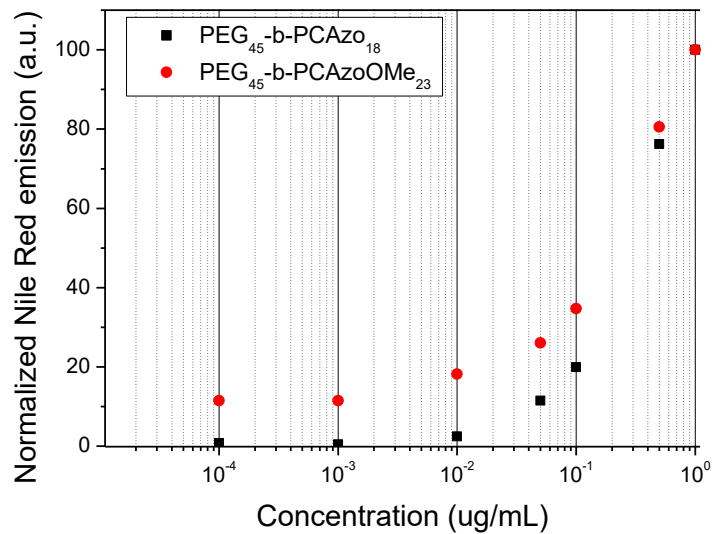


Figure S14. Normalized fluorescence emission of Nile Red at 606 nm ($\lambda_{\text{exc}} = 550 \text{ nm}$) versus the PEG₄₅-b-PCAzo₁₈ and PEG₄₅-b-PCAzoOMe₁₈ concentration. CAC was determined from the intersection of the two extrapolated lines.

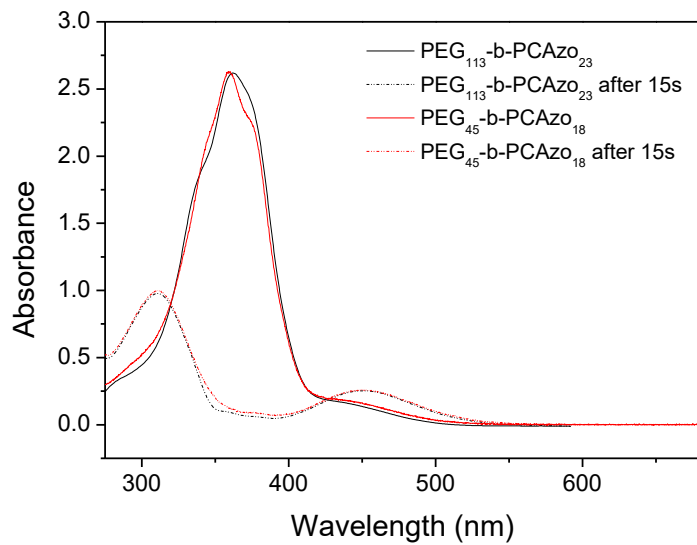


Figure S15. UV-Vis spectra of a 10^{-4} M (referred to the repetitive azobenzene unit) PEG₁₁₃-*b*-PCAzo₂₃ and PEG₄₅-*b*-PCAzo₁₈ solution in THF, before and after 15 s UV illumination.

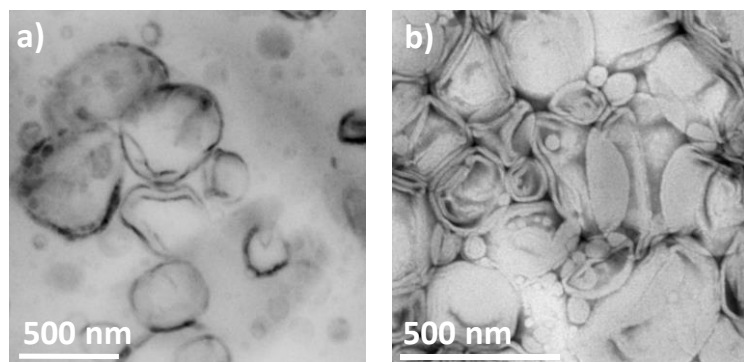


Figure S16. TEM images of PEG₄₅-*b*-PCAzo₁₈ self-assemblies before (a) and after 10 min low intensity UV light irradiation (b).

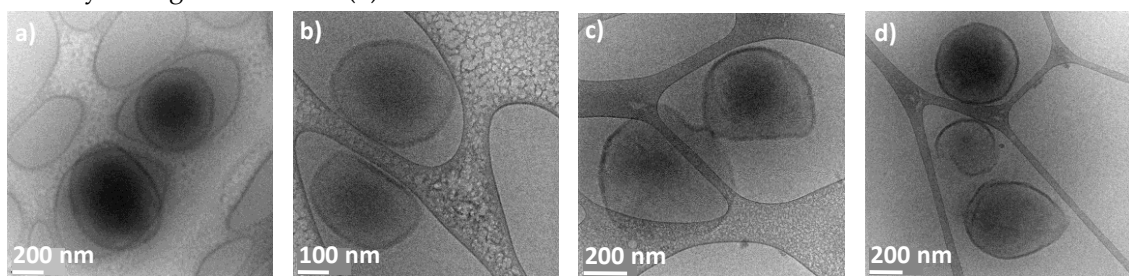


Figure S17. Cryo-TEM images of PEG₄₅-*b*-PCAzo₁₈ self-assemblies before (a and b) and after 10 min low intensity UV light irradiation (c and d).

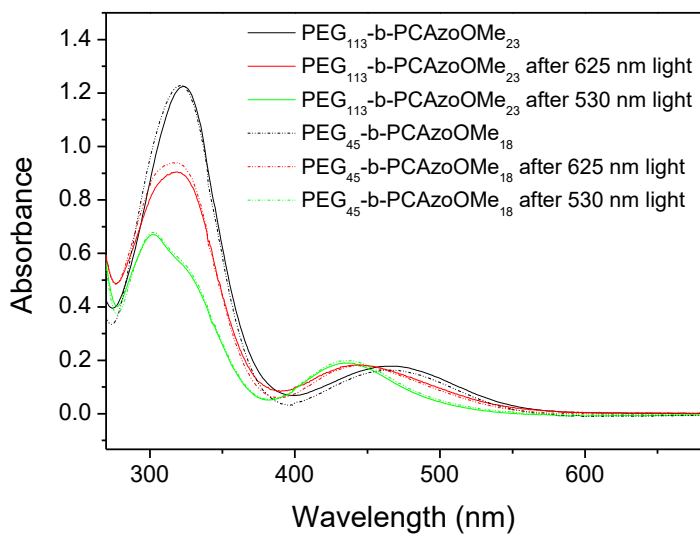


Figure S18. UV-Vis spectra of a 10^{-4} M (referred to the repetitive azobenzene unit) $\text{PEG}_{113}\text{-}b\text{-PCAzO}(\text{OMe})_{23}$ and $\text{PEG}_{45}\text{-}b\text{-PCAzO}(\text{OMe})_{18}$ solution in THF and photostationary state reached after 40 min under 625 nm light and after 30 s under 530 nm light.

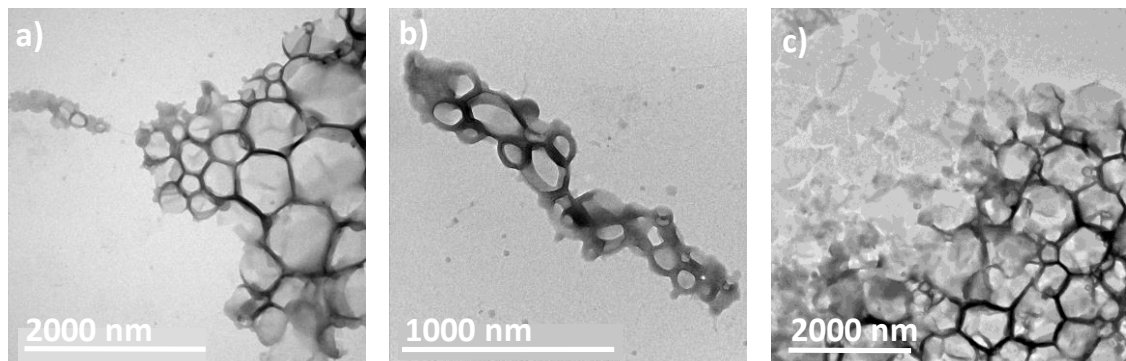


Figure S19. TEM images of $\text{PEG}_{45}\text{-}b\text{-PCAzO}(\text{OMe})_{18}$ self-assemblies before (a), after 2 hours 625 nm light irradiation (b) and after 5 min 530 nm light irradiation (b).

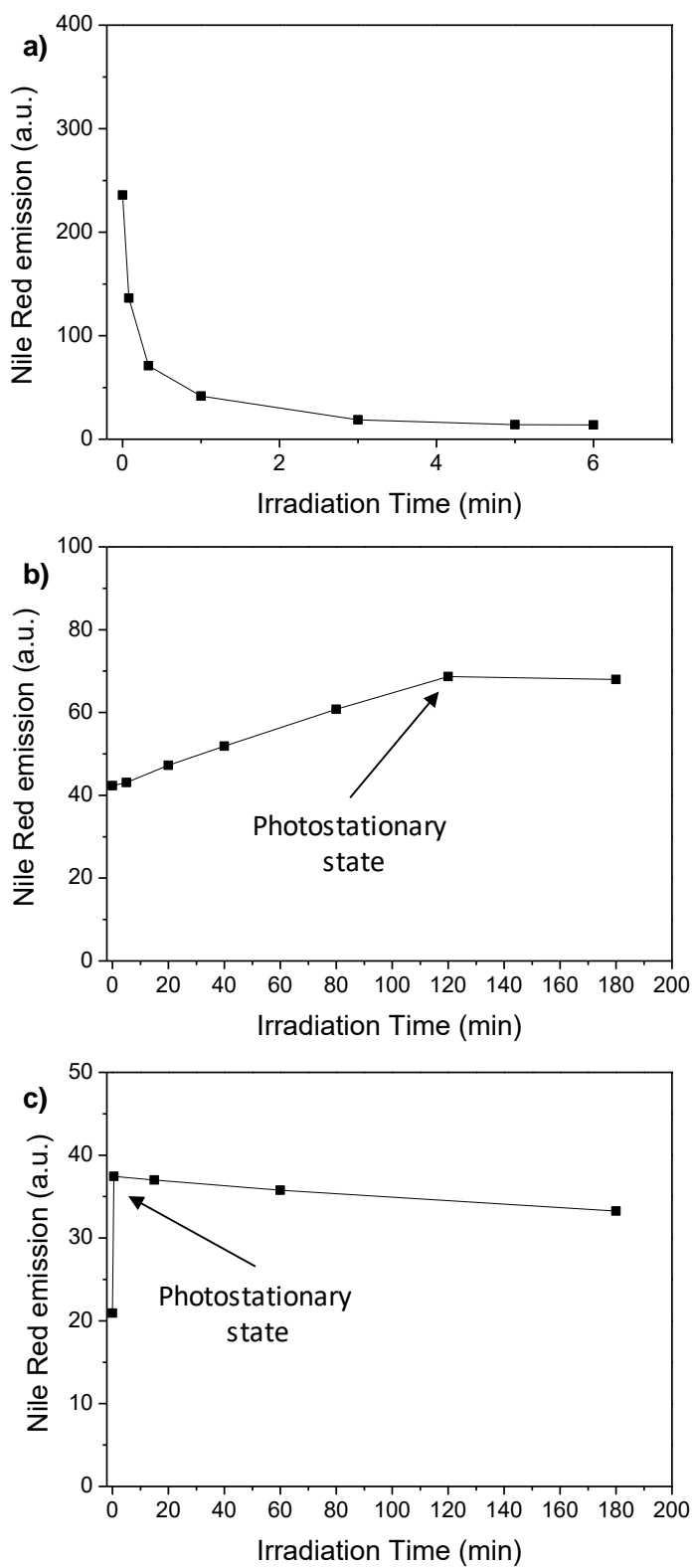


Figure S20. Cargo release profiles of the Nile Red loaded micelles for (a) $\text{PEG}_{113}\text{-}b\text{-PCAzO}_{23}$ micelles under UV light, (b) $\text{PEG}_{113}\text{-}b\text{-PCAzOOME}_{23}$ micelles under 625 nm light and (c) $\text{PEG}_{113}\text{-}b\text{-PCAzOOME}_{23}$ micelles under 530 nm.

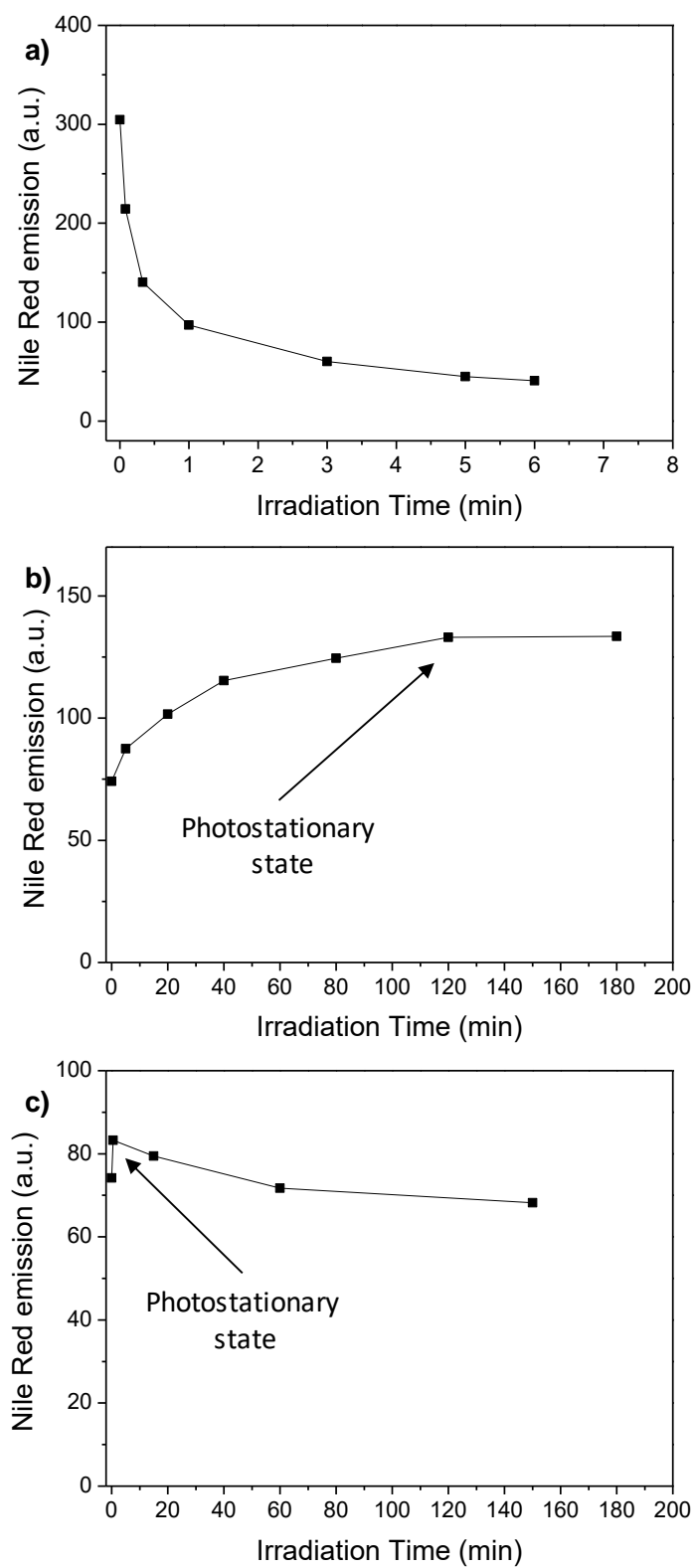


Figure S21. Cargo release profiles of the Nile Red loaded micelles for (a) $\text{PEG}_{45}\text{-}b\text{-PCAzo}_{18}$ vesicles under UV light, (b) $\text{PEG}_{45}\text{-}b\text{-PCAzoOMe}_{18}$ vesicles under 625 nm light and (c) $\text{PEG}_{45}\text{-}b\text{-PCAzoOMe}_{18}$ vesicles under 530 nm.

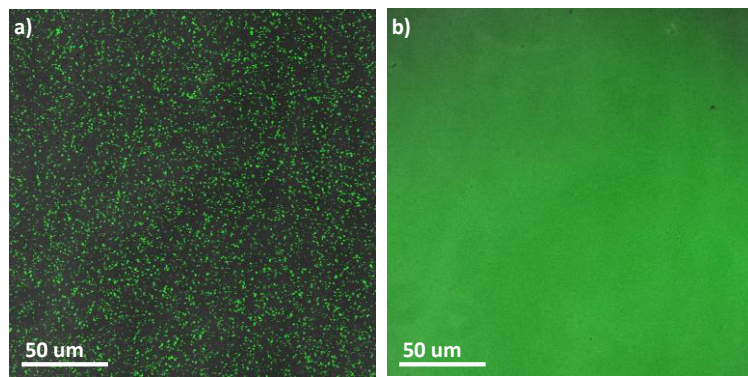


Figure S22. Fluorescence microscopy images of Rhodamine B loaded PEG₄₅-*b*-PCAzo₁₈ vesicles before (a) and after 10 min low intensity UV light irradiation (b).

Bibliography

1. Blasco, E.; Barrio, J. del; Sánchez-Somolinos, C.; Piñol, M.; Oriol, L. Light induced molecular release from vesicles based on amphiphilic linear-dendritic block copolymers. *Polym. Chem.* **2013**, *4*, 2246–2254.
2. Wang, G.; Yuan, D.; Yuan, T.; Dong, J.; Feng, N.; Han, G. A visible light responsive azobenzene-functionalized polymer: Synthesis, self-assembly, and photoresponsive properties. *Journal of Polymer Science Part A: Polymer Chemistry* **2015**, *53*, 2768–2775.
3. Blasco, E.; Barrio, J. del; Piñol, M.; Oriol, L.; Berges, C.; Sánchez, C.; Alcalá, R. Azobenzene-containing linear–dendritic block copolymers prepared by sequential ATRP and click chemistry. *Polymer* **2012**, *53*, 4604–4613.